Title
Ribulose bisphosphate carboxylase: a two-layered, square-shaped molecule of symmetry 422.

Journal
Science (New York, N.Y.), 196(4287)

ISSN
0036-8075

Authors
Baker, TS
Eisenberg, D
Eiserling, F

Publication Date
1977-04-01

DOI
10.1126/science.196.4287.293

Peer reviewed

Ribulose Bisphosphate Carboxylase: A Two-Layered, Square-Shaped Molecule of Symmetry 422

Abstract. *Electron micrographs and x-ray diffraction patterns of crystals of ribulose bisphosphate carboxylase, probably the most abundant protein on earth, have provided new details of the arrangement of subunits. The eight large subunits and eight small subunits are clustered in two layers, perpendicular to a fourfold axis of symmetry. Viewed down the fourfold axis, the molecule is square-shaped.*

Electron micrographs and x-ray diffraction from a new crystal form of D-ribulose-1,5-bisphosphate carboxylase (RuBPCase) show much about the arrangement of subunits in the molecule. RuBPCase initiates the Calvin cycle of photosynthesis and is probably the most abundant protein on earth (*1*). In green plants, the enzyme is found inside the chloroplast, sometimes in crystalline form (*1, 2*). The enzyme can also be crystallized in vitro (*3*). Our study of crystal form I of the in vitro crystals yielded a preliminary picture of the subunit organization of the molecule. The 560,000-dalton enzyme contains eight large (L) (about 55,000 daltons) and eight small (S) (about 15,000 daltons) subunits, and displays one cylindrical hole of about 20 Å in diameter that runs through the molecule. The subunits are arranged with a minimum D_2 (222) symmetry; that is, the polypeptide chains are packed around three mutually perpendicular twofold rotation axes. Electron micrographs of a new crystal form, II, show images of the molecules in which some substructure is visible. X-ray diffraction and related measurements on form II show that the eight LS subunit pairs are organized in a two-layer molecule with D_4 (422) symmetry.

Crystal form II of RuBPCase from tobacco is grown by the same procedure as form I (*4*), except that dialysis of the protein solution (5 to 10 mg/ml) is carried out in 0.05*M* potassium phosphate buffer at *p*H 6.0. Two crystal morphologies are obtained: large (0.2 to 0.7 mm), birefringent triangular prisms suitable for x-ray diffraction experiments, and thin (~ 0.1 μm) square platelets suitable for electron microscopy.

X-ray precession photographs of the *hk*0 (Fig. 1, A and B) and *h*0*l* (not shown) zones of form II reveal that the crystal system is tetragonal with unit cell dimensions $a = b = 230 \pm 2$ Å, and $c = 315 \pm 3$ Å. Optical diffraction patterns (Fig. 1, C and D) from electron micrographs also reveal two perpendicular cell edges of 230 Å. Both x-ray and optical diffraction patterns show that the structure at very low resolution (~ 80 Å) has unit cell dimensions $a = b = 162$ Å. At higher resolution (15 to 80 Å; Fig. 1, B and D) the space group is $P42_12$ as determined from the reciprocal lattice symmetry (4/*mmm*) and systematically absent reflections.

In determining the arrangement of molecules within this unit cell we were aided by the micrograph of a negatively stained platelet that is reproduced in Fig. 2. This micrograph is also the first one that we obtained in which some molecular substructure of RuBPCase is visible (see below). The view is down the *c*-axis, and the dominant feature is an array of square-shaped (~ 114 by 114 Å) molecules apparently arranged on a 162-Å square lattice. Nearly every molecule contains a hole ~ 20 Å in diameter oriented parallel to the *c*-axis. The molecules are separated from neighbors by dark strips of negative stain, and at first inspection it is difficult to see how the crystal can be self-supporting, that is, how molecules adhere to one another. Close examination of the original negative, however, reveals molecules obscured by stain, centered in projection among each four molecules of the 162-Å square lattice. These obscured molecules show up on a very underexposed print of the negative (Fig. 2C).

We can explain this uneven imaging of molecules by assuming that the platelet is only one unit cell in thickness. Each "clear molecule" could then be a projection through two molecules, whereas each "obscured molecule" could be a projection through one molecule plus stain. In other words, one-third of the molecules are obscured because they are covered with a thicker layer of stain. Just such an arrangement is possible in space group $P42_12$, if we assign the obscured molecules to special positions *c* (of symmetry 4) in the Wyckoff notation and the clear molecules to special positions *d* (of symmetry 2) (*5*). This requires, however, that there are six molecules per unit cell, rather than the four or eight that might be expected in this space group.

For this reason, we carefully determined *n*, the number of molecules per unit cell, from the well-known relationship $[N \rho V(\bar{\nu}_s - 1/\rho)]/[M(\bar{\nu}_s - \bar{\nu}_p)]$, in which *N* is Avogadro's number, ρ is the crystal density, *V* is the unit cell volume, *M* is the molecular weight of the enzyme,

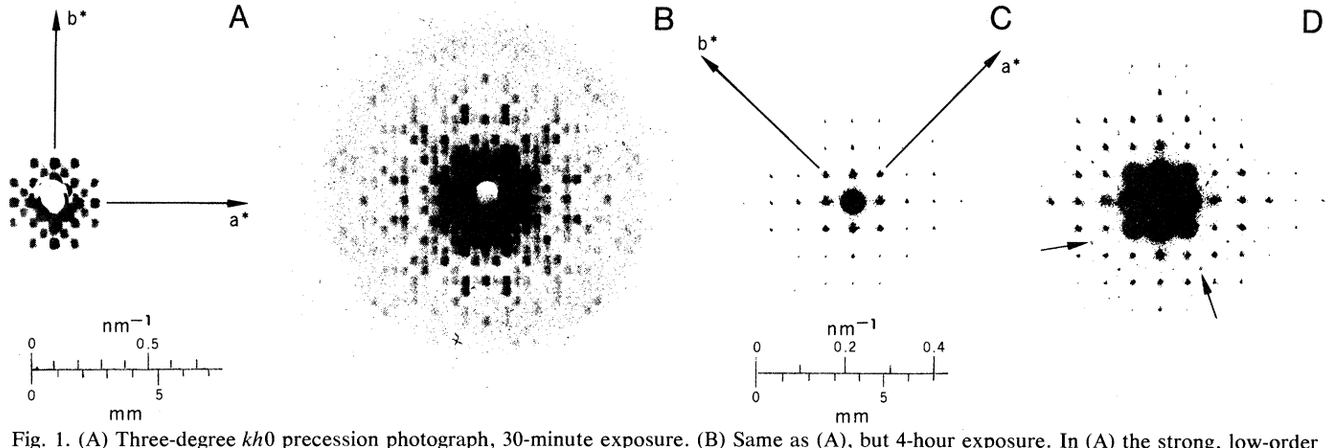

Fig. 1. (A) Three-degree *kh*0 precession photograph, 30-minute exposure. (B) Same as (A), but 4-hour exposure. In (A) the strong, low-order reflections form a pseudo lattice (1/162 Å by 1/162 Å). In (B) the pattern extends to 14.8 Å and reveals the true lattice dimensions (1/230 Å by 1/230 Å). The photographs were recorded as described (*4*). The scale is the same for (A) and (B). (C) Optical diffraction pattern from the circular region in Fig. 2A, with an exposure time of 0.125 second. The low-order reflections form a 1/162-Å square lattice. (D) Same as (C), but with an exposure time of 8 seconds. The true lattice dimensions (1/230 Å by 1/230 Å) are revealed by the presence of weak reflections (indicated by arrows) appearing at centered points in the pseudo lattice.

$\bar{v}_s$ is the partial specific volume of the liquid of crystallization, and $\bar{v}_p$ is the partial specific volume of the protein in the crystal. The wet densities of ten crystals were measured on a bromobenzene-xylene column (*6*), and gave an average value of $\rho = 1.095 \pm 0.006$ g/cm^3. The partial specific volume of liquid of crystallization ($\bar{v}_s = 0.9977 \pm 0.0020$ cm^3/g) was estimated by measuring the density of the mother liquor. The partial specific volume of the protein ($\bar{v}_p = 0.734 \pm$

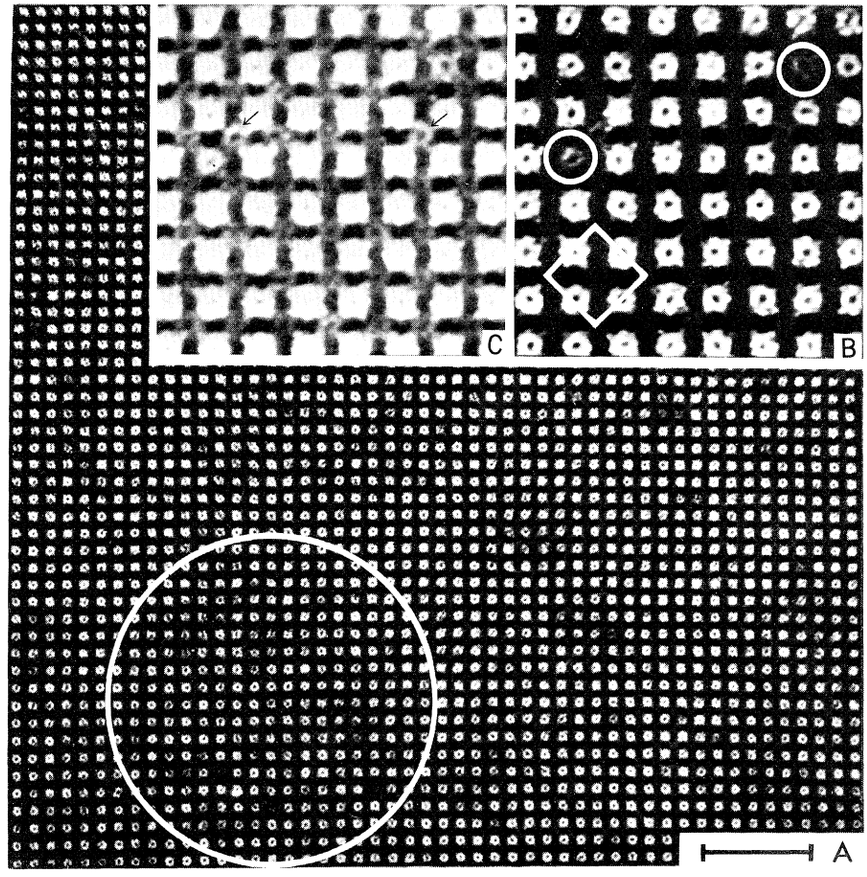

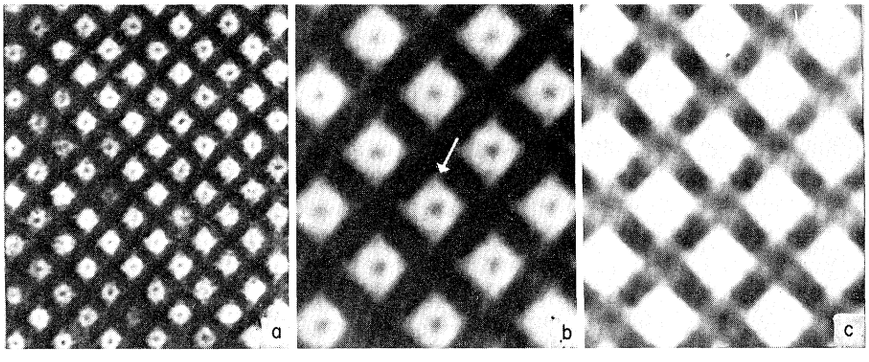

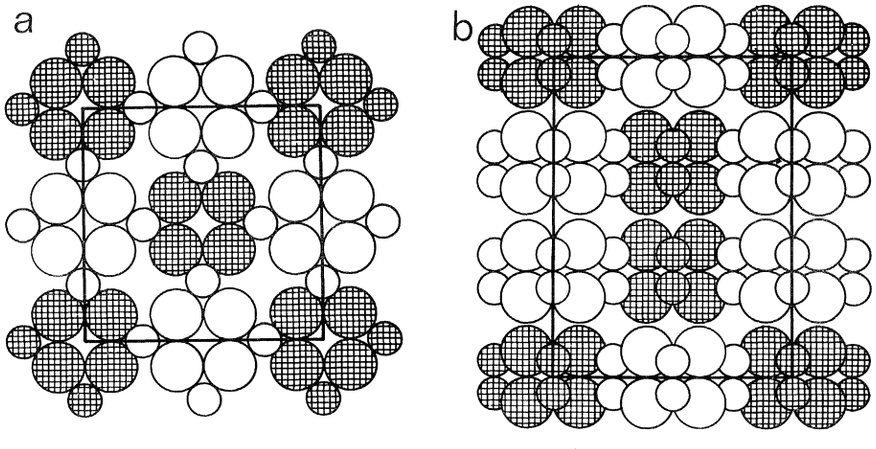

Fig. 2 (top). (A) Electron micrograph, recorded by methods described (*4*) of a thin form II RuBPCase crystal revealing a square array of molecules separated by dark strips of stain. The circular area outlined at the lower left was further processed by optical diffraction and filtering. The scale bar represents 100 nm. The packing scheme proposed in the text implies that this micrograph does not accurately portray the distribution of protein (stain excluding material) in the projected structure. If an integral number of unit cells is evenly contrasted by stain, then the "obscured" molecules (C) should appear half as bright as the clear molecules (A) and (B), and the intensity of the 162-Å (1, 1) reflection should be less than the 115-Å (2, 0) reflection (Fig. 1D). This is not true in Fig. 1. Other platelet micrographs in which the crystal is contrasted more evenly and optical diffraction patterns show that the 2, 0 type reflections are more intense than the 1, 1 type reflections. Unfortunately these other micrographs are confusing because of superposition of additional layers of molecules. (B) The enlarged region shows detail in individual molecules. One unit cell (230 by 230 Å) is outlined. Circles indicate defects in the crystal where presumably single molecules were either lost or excluded during crystal growth. Faint images of molecules do appear in these positions, indicating that the strong molecular images arise from superposition of more than one molecule (*9*). (C) Same as (B), but the print was underexposed to reveal the additional molecules obscured by the strips of stain (arrows point to two of these). These obscured molecules are squarish, and in projection are positioned among the four clear molecules situated on the 162-Å square lattice. There is little indication for stain excluding material in the region between clear molecules. Fig. 3 (middle). Optical reconstructions from an identical region of the micrograph in Fig. 2: (a) unfiltered reconstruction; (b) enlarged region of the filtered reconstruction; (c) same as (b), but the print is underexposed to show the filtered appearance of "obscured" molecules. Filtering was accomplished by allowing all reflections on the 1/230-Å lattice to pass through holes etched in a copper mask positioned in the transform plane of the diffractometer. The size of the holes (0.2 mm) was selected so as to produce a reconstruction in which one filtered unit cell results from averaging the information contained in approximately 24 molecules. In (b) and (c), the averaged molecules are seen, and the arrow in (b) points to a spike at the corner of a molecule. Fig. 4 (bottom). Packing of RuBPCase molecules in crystal form II. Each molecule contains eight large and eight small subunits, arranged in symmetry D_4 (422). Large subunits are represented by large spheres, and small subunits by small spheres. The positions of the small subunits are conjectural. (a) View of crystal parallel to the *c*-axis. Light molecules correspond to the "clear" molecules of Fig. 2 and shaded molecules to the "obscured" molecules. (b) View of crystal parallel to the *a*-axis.

0.010 cm^3/g) was estimated by Kwok (*7*) from the amino acid composition. For the molecular weight, we adopt the most commonly reported value (*8*) and assign to it a generous error (M = 560,000 ± 25,000). With these estimates we find that n is 6.3 ± 0.5. If the estimates of errors in all quantities are doubled, the resulting error is ± 0.8. If the estimated error in molecular weight is doubled and all other errors quadrupled, n = 6.3 ± 1.2. Thus it is unlikely that there are eight molecules per cell and very unlikely that there are four.

The evidence for six molecules per unit cell, rather than two, four, or eight, is supported by intensities of reflections on the *h*0*l* zone of the x-ray pattern. Along the 0,0,*l* line [*c*-axis (*9*)], the 0,0,3; 0,0,6; and 0,0,12 reflections are strong, but the 0,0,4 reflection is weak. This implies that, at very low resolution, the structure when viewed along the *a*- or *b*-axis is composed of three layers of electron-dense material (RuBPCase molecules). Moreover, the exceedingly strong 0,0,6 reflection is consistent with the notion that each molecule is itself a double-layered structure (see below). A unit cell with two or four layers of molecules is not compatible with these intensities, nor are such cells consistent with the *c*-axial dimension (which is roughly three times the observed molecular diameter of 115 Å) (*4*).

By combining information from both the form I and form II crystals, we can determine the symmetry of the RuBPCase molecule. Our study of form I crystals (*4*) showed that RuBPCase molecules have a minimum symmetry of three mutually perpendicular twofold axes (D_2 = 222). Similarly, the six molecules per unit cell in the form II crystals, must occupy special positions of defined symmetry. Two of the molecules contain at least a fourfold axis of rotation, and the remaining four contain at least a twofold axis. If we assume that all molecules are identical, then the combined symmetries of D_2 (222) and C_4 (*4*) in the two crystal forms demand that the RuBPCase molecule has D_4 (422) symmetry. This is the highest symmetry that an L_8S_8 oligomer can possess, and it is the symmetry expected for a self-assembling aggregate of this stoichiometry.

The filtered reconstruction of Fig. 3 contains some additional information on subunit structure. Each molecule in the filtered images (Fig. 3, b and c) is averaged with ~ 24 equivalent neighboring molecules. The filtered molecules are squarish in outline and appear to contain a fourfold rotation axis coincident with the hole. Four elliptical units appear bonded in a square planar ring with four faint spikes of density (arrow, Fig. 3b) at the intersections of denser units. The filtering procedure has slightly enhanced the presence of the molecules obscured by stain (Fig. 3c).

From these filtered images and from the molecular symmetry, we propose a model of RuBPCase quaternary structure: the molecule is double layered, with each layer comprised of a ring of four large, elliptical subunits. The two layers are nearly eclipsed as suggested by the images in electron micrographs, even though this is not required by symmetry. The spikes at the corners of the square molecules (arrow, Fig. 3b) may conceivably be the small subunits, or the spikes may result from the superposition of parts of the obscured molecules with the clear molecules. Figure 4 depicts this model schematically, showing the arrangement of molecules in the form II crystals.

TIMOTHY S. BAKER
DAVID EISENBERG
FREDERICK EISERLING
Departments of Chemistry and *Bacteriology* and *Molecular Biology Institute, University of California, Los Angeles 90024*

References and Notes

1. S. G. Wildman, K. Chen, J. C. Gray, S. D. Kung, P. Kwanyuen, K. Sakano, in *Genetics and Biogenesis of Chloroplasts and Mitochondria*, P. S. Perlman, C. W. Birky, T. J. Byers, Eds. (Ohio State Univ. Press, Columbus, 1975), chap. 9; I. Takebe and Y. Otsuki, *Planta* **113**, 21 (1973); B. E. S. Gunning, M. W. Steer, M. P. Cochrane, *J. Cell Sci.* **3**, 445 (1968); M. Wrischer, *ibid.* **75**, 309 (1967); C. Larsson, C. Collin, P. A. Albertsson, *J. Ultrastruct. Res.* **45**, 50 (1973).
2. L. K. Shumway, T. E. Weier, C. R. Stocking, *Planta* **76**, 182 (1967).
3. P. J. Chan, K. Sakano, S. Singh, S. G. Wildman, *Science* **176**, 1145 (1972); R. Chollet, L. L. Anderson, L. C. Hovespian, *Plant Physiol.* **56** (Suppl.), 26 (1975).
4. T. S. Baker, D. Eisenberg, F. A. Eiserling, L. Weissman, *J. Mol. Biol.* **91**, 391 (1975).
5. N. F. M. Henry and K. Lonsdale, in *International Tables for X-ray Crystallography* (Kynock, Birmingham, England, ed. 3, 1969), vol. 1, p. 180.
6. B. W. Low and F. M. Richards, *J. Am. Chem. Soc.* **76**, 2511 (1954).
7. S. Y. Kwok, thesis, University of California, Los Angeles (1972).
8. M. I. Siegel, M. Wishnick, M. D. Lane, in *The Enzymes*, P. D. Boyer, Ed. (Academic Press, New York, ed. 3, 1972), vol. 6, pp. 169–192.
9. In the proposed packing, these single "defect" molecules should appear with the same brightness as the "obscured" molecules. In fact they are brighter. This could arise from any of the following: (i) A nonintegral number of unit cells in this platelet; (ii) uneven wetting of stain (for example, the defect molecules could simply be normal molecules with a bit of dried stain on top); or (iii) unequal affinity of stain for the crystallographically nonequivalent positions occupied by "obscured" and "defect" molecules.
10. We acknowledge with thanks support from PHS, NSF, and the Research Corporation, and also the help of K. Chen in obtaining pure enzyme.

13 July 1976; revised 12 November 1976

High Rates of Vertical Crustal Movement near Ventura, California

Abstract. *Fission track, radiometric, and paleomagnetic age determinations in marine sedimentary rocks of the Ventura Basin make it possible to estimate the vertical components of displacement rates for the last 2 million years. The basin subsided at rates up to 9.5 ± 2.5 millimeters per year until about 0.6 million years ago, when subsidence virtually ceased. Since then, the northern margin of the basin has been rising at an average rate of 10 ± 2 millimeters per year, about the same rate as that based on the geodetic record north and west of Ventura since 1960 but considerably lower than the rate along the San Andreas fault at Palmdale since 1960.*

The Ventura Basin has long been known for its thick sedimentary sequence of late Cenozoic age, which was strongly deformed during the Pleistocene (*1*). This sequence consists of deep-water sandstones and siltstones of the Fernando Formation overlain conformably by the shallow-marine and nonmarine Saugus Formation, which is itself overlain unconformably by alluvial deposits including the Mugu and Oxnard aquifers. The marine part of this sequence is highly fossiliferous, but the provinciality of the fossil assemblages precludes precise correlation with worldwide Cenozoic stages calibrated in radiometric ages. Recently, however, the Bailey ash bed midway in the Fernando-Saugus sequence was dated as 1.2 ± 0.2 million years by the fission-track method on zircon (*2*), and paleomagnetic stratigraphy of the Saticoy oil field was used to identify the Olduvai and Jaramillo normal events of the Matuyama reversed epoch (*3*). Constraints on the minimum age of the Saugus Formation are provided by the ages of two biostratigraphically distinct sets of marine terraces along the California coast as determined by uranium-series methods (*4*) and amino acid racemization (*5*); these ages are 0.09 and 0.13 million years, respectively, with a considerable margin of error. A similar but undated set of marine terraces north and west of the city of Ventura truncates the south-dipping Saugus Formation (*6*). Uplift rates in the Santa Monica Mountains based on the dated terraces there led